coatings

MDPI

Article

Discoloration Resistance of Electrolytic Copper Foil Following 1,2,3-Benzotriazole Surface Treatment with Sodium Molybdate

Dong-Jun Shin [1,2,†], Yu-Kyoung Kim [3,†], Jeong-Mo Yoon [1] and Il-Song Park [1,*]

[1] Division of Advanced Materials Engineering, Research Center for Advanced Materials Development and Institute of Biodegradable Materials, Chonbuk National University, Jeonju 561-756, Korea; dongjun519@naver.com (D.-J.S.); yoonjm@jbnu.ac.kr (J.-M.Y.)
[2] Graduate School of Engineering, Tohoku University, Sendai 980-8579, Japan
[3] Department of Dental Biomaterials, Institute of Biodegradable Materials, BK21 plus Program, School of Dentistry, Chonbuk National University, Jeonju 561-756, Korea; yk0830@naver.com
* Correspondence: ilsong@jbnu.ac.kr; Tel.: +82-63-270-2294
† These authors contributed equally to this study.

Received: 26 October 2018; Accepted: 20 November 2018; Published: 26 November 2018

Abstract: The copper which an important component in the electronics industry, can suffer from discoloration and corrosion. The electrolytic copper foil was treated by 1,2,3-benzo-triazole (BTA) for an environmentally friendly non-chromate surface treatment. It was designed to prevent discoloration and improve corrosion resistance, consisted of BTA and inorganic sodium molybdate (Na_2MoO_4). Also the ratio of the constituent compounds and the deposition time were varied. Electrochemical corrosion of the Cu-BTA was evaluated using potentiodynamic polarization. Discoloration was analyzed after humidity and heat resistance conditioning. Surface characteristics were evaluated using scanning electron microscopy (SEM) and X-ray photoelectron spectroscopy (XPS). Increasing corrosion potential and decreasing current density were observed with increasing Na_2MoO_4 content. A denser protective coating formed as the deposition time increased. Although chromate treatment under severe humidity (80% humidity, 80 °C, 100 h) provided the highest humidity resistance, surface treatment with Na_2MoO_4 had better heat discoloration inhibition under severe heat-resistant conditions (180 °C, 10 min). When BTA reacts with Cu to form the Cu-BTA-type insoluble protective film, Na_2MoO_4 accelerates the film formation without being itself adsorbed onto the film. Therefore, the addition of Na_2MoO_4 increased anticorrosive efficiency through direct/indirect action.

Keywords: electrolytic copper foil; 1,2,3-benzotriazole; inorganic sodium molybdate (Na_2MoO_4); electrochemical corrosion; discoloration; insoluble protective film

1. Introduction

The copper is an important component in the electronics industry owing to its superior heat conductivity, electrical conductivity and workability. Copper foils with thicknesses of 5–100 μm are used for wiring the electronic circuits of printer and battery electrodes [1]. Recently, the materials used in electronic components are becoming thinner, simpler, more complex and highly functional with the rapid development of the electronic information industry. Since the rolled copper foil is susceptible to cyclic strain hardening and fatigue [2,3], thinner electrolytic copper foil is increasingly being used. Both copper foils are usually manufactured using a sulfuric acid-copper sulfate electrolytic solution. Electrolytic copper foil has the advantages of faster production speed, lower cost, constant strength and greater flexibility of the thin film [4]. However, electrolytic copper foil produced using plating baths is easily oxidized and suffers from surface discoloration in humid environments [5–7].

This discoloration and corrosion results in reduced adhesive strength and a failure of the electrical conductivity when applied to a PCB (Printed Circuit Board) substrate. Therefore, post-treatment (e.g., chromate immersion) is used during the production of electrolytic copper foil to provide resistance to discoloration and corrosion resistance [8,9] and to improve adhesion [10]. Chromate treatment contains hexavalent chromium and reducing trivalent chromium, both of which are designated as environmentally hazardous elements in the restriction of hazardous substances (EU RoHS). Their usage and surface-treatment content are subject to strict international restrictions and controls [11]. Therefore, research related to the development of new rust-preventive materials and processing technologies is needed.

In previous studies, materials for enhancing the rust-prevention effect of copper or copper alloys have been heterocyclic compounds, containing large numbers of N and S atoms, that form a physical barrier on the copper surface [12], or a-based compounds of benzotriazole containing large amounts of C, H and N atoms [13,14]. For example, benzotriazole (BTA) has been reported to have excellent antirust qualities when it forms an insoluble compound in the form of Cu-BTA on the copper surface. This physical protective film inhibits the diffusion of permeable ions such as P, S and Cl [13,15]. However, alone, it cannot match the tarnish-inhibitive properties of chromate and many studies have used a combination of organic and inorganic compounds with BTA to improve the rust-prevention effect of the surface treatment [16–19]. In particular, the addition of potassium-sorbate [18] or sodium-dodecylsulfate [19] has been reported to increase the adsorption rate of BTA onto the copper surface and to improve corrosion resistance by forming a thicker Cu-BTA film. Molybdate (MoO_4) is known to provide corrosion resistance when mixed with organic materials owing to its non-oxidative property [20–22]. It has been applied as a corrosion inhibitor for copper-coupled steel [23]. The addition of sodium molybdate (Na_2MoO_4) to low-concentration solutions is often used in combination with other inhibitors because it accelerates corrosion resistance due to oxidation [24]. Ramesh [22] reported the rust-inhibition effect for copper by mixing a triazole compound with molybdate but relatively few studies have considered the complex anti-rusting effect of BTA and molybdate [16,25].

In this study, copper foil surface treatment was performed by adding Na_2MoO_4 to BTA. The results showed that this pretreatment improved corrosion and discoloration resistance and an optimum pretreatment procedure was developed by varying the concentrations of additives and deposition time.

2. Materials and Methods

Untreated copper foil (Iljin Copper Foil Co., Ltd., Iksan, Korea), with a thickness of 12 μm, was cut into 30 mm × 50 mm pieces and subjected to surface treatment. Commercialized chromate copper (Iljin Copper Foil Co., Ltd., Korea) foil was used for comparison [26]. The copper foil was pickled in a 20 vol.% H_2SO_4 aqueous solution to remove the oxide film formed by contact with the atmosphere. The electrolyte was prepared as 5 and 50 mM BTA (1,2,3-benzotriazole, $C_6H_5N_3$) without Na_2MoO_4 and 1 and 5 mM of Na_2MoO_4 was added in 5 and 50 mM BTA (1,2,3-benzotriazole, $C_6H_5N_3$), respectively. The copper foils was immersed for 3 or 5 s in one of the two surface-treatment solutions. The concentrations of BTA and Na_2MoO_4 and the surface-treatment time conditions are summarized in Table 1.

To investigate the electrochemical properties, potentiodynamic polarization tests were performed with EG&G PAR (273A, Princeton Applied Research Corporation, Princeton, NY, USA). A test sample was used as a working electrode and Pt was connected to a counter electrode. Ag/AgCl (saturated KCl) was used as a reference electrode at 3 mV/s in 3.5 wt.% NaCl solution. Potential corrosion and current density were measured by Tafel extrapolation to evaluate the electrochemical corrosion characteristics. The test was performed 5 times and the mean and standard deviation were obtained.

Table 1. Experimental conditions.

Sample Code		BTA (mM)	Sodium-Molybdate (mM)	Surface Treatment Time (s)
Comparison Groups	Untreated	–	–	–
	Chromate	–	–	–
Modified Groups	B5	5	–	3/5
	B5M1	5	1	
	B5M5	5	5	
	B50	50	–	
	B50M1	50	1	
	B50M5	50	5	

Evaluation of discoloration resistance of the surface-treated specimens was carried out under severe high-temperature (heat resistance) and humidity (moisture resistance) environments. To evaluate discoloration at high temperatures, the samples were exposed to a constant temperature of 180 °C for 10 min. Discoloration in humid environments was evaluated by exposing the specimen to 80% humidity at 80 °C for 100 h. To prevent local corrosion, each sample was held at least 30 mm from the ground and the intersample distance was maintained at 50 mm to control interferences between the samples. The coloration of the electrolytic copper foil was analyzed using a colorimeter (Color i5, X-rite, Grand Rapids, MI, USA). A D65 light source was chosen for analyzed according to the guidelines of the Commission Internationale de I'Eclairage (CIE) and the values of color coordinates L^*, a^* and b^* were measured with a viewing angle of 2° using the SCE (Specular Component Excluded) method. The average mean value of L^*, a^* and b^* was obtained by measuring the center of the sample 10 times to calculate a ΔE^* value. The color coordinates were derived using the equation:

$$\Delta E^* = [(\Delta L^*)^2 + (\Delta a^*)^2 + (\Delta b^*)^2] \quad (1)$$

where $\Delta L^* = L_1^* - L_2^*$, $\Delta a^* = a_1^* - a_2^*$ and $\Delta b^* = b_1^* - b_2^*$. L_1^*, a_1^* and b_1^* represent values before harsh condition testing of the surface-treated sample and L_2^*, a_2^* and b_2^* represent values after harsh condition testing. Discoloration resistance data were analyzed for statistical significance using a one-way ANOVA-test which a p value of less than 0.05 was considered significant. After treatments and tarnish testing, surface morphology and color were observed using a stereomicroscope (DE/EZ4, Leica, Milton Keynes, UK). The thickness of the film was measured seven times and the average and standard deviation were obtained by excluding the minimum value and the maximum value.

The copper foils treated for 5 s were solidified in liquid nitrogen and then cut to observe a cross-section using FE-SEM (field emission scanning electron microscopy, SU-70, Hitachi, Tokyo, Japan).

Surface component analysis of Na_2MoO_4 concentrations was performed using X-ray photoelectron spectroscopy (XRP, Kα Model, Thermo VG Scientific, Waltham, MA, USA).

3. Results and Discussion

3.1. Characterization of Electro-Chemical Corrosion

Potentiodynamic polarization is an electrochemical method that is mainly used to measure the corrosion resistance of a material with a coating layer. The corrosion currents (I_{corr}) of the samples were determined at the intersection of the extrapolated cathodic and anodic Tafel lines using the linear polarization method. Figure 1 and Table 2 show the results of the potentiodynamic polarization of copper foil treated at 20 °C for 3 s under the addition of Na_2MoO_4. The BTA treatment groups showed higher corrosion potential and lower corrosion current than those of untreated and chromate groups. In terms of concentration polarization in hydrogen reduction, the reduction rate is dominated by the diffusion of hydrogen ions toward the metal surface [27]. The limiting diffusion current density is affected by the diffusion coefficient, the concentration of reactive ions in the solution and the thickness of the diffusion layer [28]. In this study, the diffusion coefficient and the concentration of reactive ions in solution are not different, so the change in cathodic current densities will be determined by the

thickness of the diffusion layer. Thin and dense chromate coatings of several nanometers in thickness will have relatively low cathodic polarization currents [29]. The BTA coating is less dense than the chromate treatment but it has a thick and stable coating of 60 nm or more, increasing the corrosion potential and the fitting potential at the higher potential.

Table 2. Corrosion potential and current densities from potentiodynamic polarization.

Sample Code	E_v (V)	Standard Deviation	I_{corr} (A/cm^2)	Standard Deviation (10^{-6})
Untreated	−0.278	±0.012	1.152×10^{-5}	±1.984
Chromate	−0.227	±0.008	1.906×10^{-6}	±0.331
B5(3 s)	−0.152	±0.007	2.392×10^{-6}	±2.616
B5M1(3 s)	−0.115	±0.007	6.880×10^{-7}	±0.149
B5M5(3 s)	−0.096	±0.005	7.249×10^{-7}	±0.271
B50(3 s)	−0.158	±0.007	5.336×10^{-7}	±0.099
B50M1(3 s)	−0.120	±0.006	6.469×10^{-7}	±0.151
B50M5(3 s)	−0.104	±0.011	7.223×10^{-7}	±0.143
B5(5 s)	−0.155	±0.004	3.708×10^{-7}	±0.090
B5M1(5 s)	−0.098	±0.007	1.623×10^{-6}	±0.551
B5M5(5 s)	−0.081	±0.005	3.749×10^{-7}	±0.115
B50(5 s)	−0.101	±0.005	8.213×10^{-7}	±0.245
B50M1(5 s)	−0.074	±0.009	6.505×10^{-7}	±0.203
B50M5(5 s)	−0.070	±0.036	4.357×10^{-7}	±0.135

Figure 1b shows experiments with higher BTA (50 mM) after immersion for 3 s. It was observed no differences in the corrosion current density and corrosion potential as compared with those observed for 5 mM BTA (Figure 1a). Lower corrosion current density increased the surface-insoluble coating and corrosion resistance. Although increasing the amount of Na_2MoO_4 had a positive effect on corrosion resistance, the corrosion potentials and current densities of 5 and 50 mM BTA concentrations did not show significant differences. There is a threshold value of BTA ion concentration for the reaction to form an insoluble Cu-BTA film during the reaction of BTA and copper. It was observed that the copper removal rate gradually increased with higher BTA concentrations, when BTA addition was lower than 2 mM, a uniform and compact Cu-BTA passivating film could not be effectively built up [30]. Finsgar [31] considered BTA concentrations of 0.1–10 mM and found that rust-inhibition efficiency decreased with the addition of more than 10 mM BTA during co-electrospinning potential in 3% NaCl solution.

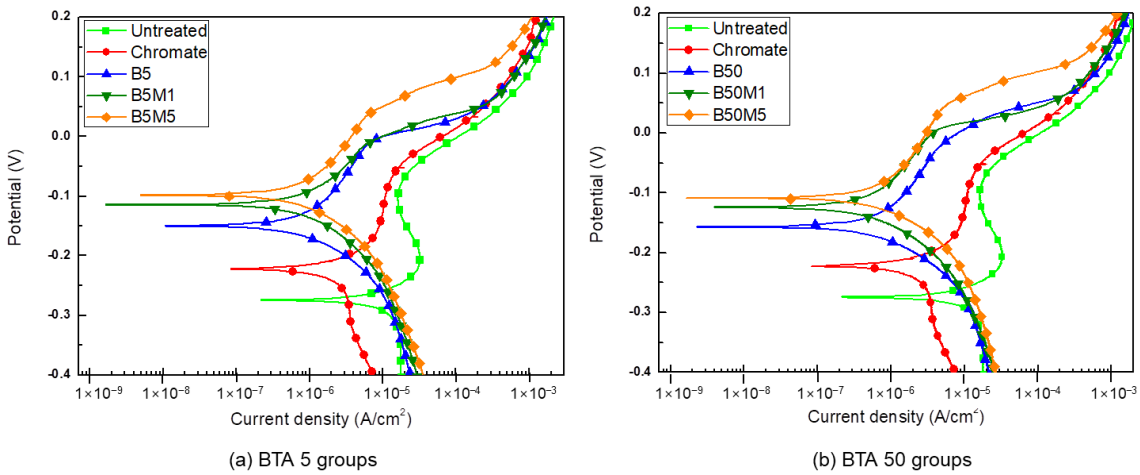

Figure 1. Potentiodynamic polarization curves of surface treatment immersed for 3 s in (**a**) 5 mM and (**b**) 50 mM 1,2,3-benzotriazole (BTA) combined with sodium molybdate (Na_2MoO_4).

Figures 1 and 2 and Table 2 show potentiodynamic polarization as a function of surface-treatment time. The corrosion resistances of 5 mM BTA concentration did not change with surface-treatment time

(3 s or 5 s; Figures 1a and 2a). However, the corrosion potentials increased by the addition of Na_2MoO_4. For a treatment time of 5 s, the 50 mM BTA groups had a higher potential voltage than did the 5 mM BTA groups. Therefore, the increase in the corrosion potential was proportional to the immersion time and to the addition of high amounts of BTA and Na_2MoO_4. However, the addition of more than 1 mM Na_2MoO_4 resulted in reduced potential voltage (Figure 2b). Increasing the amount of Na_2MoO_4 (i.e., over 5 mM) did not affect the rate of corrosion, because Na_2MoO_4 at 0.01 M concentration in the electrolyte represents a critical quantity for stable passivation [32]. The presence of molybdate results in the passivation of copper, which enhances the adsorption of BTA [25]. Moshier et al. [33] showed that both the Mo +4 and Mo +6 states is limited by solubility and the molybdate had been reduced during the formation of the passive film. However, a certain amount of molybdenum concentration does not increase the film. In other words, just 1 mM of molybdate anions in the solution is sufficient to quickly absorb the surface and form a thin MoO_2 film and that film growth is controlled by the diffusion of anions. In this study, the critical amount of Na_2MoO_4 of copper foil was identified to improve corrosion resistance. For Q235 steel, Zhou et al. [34] found that the optimum ratio of Na_2MoO_4 to BTA is 4:1.

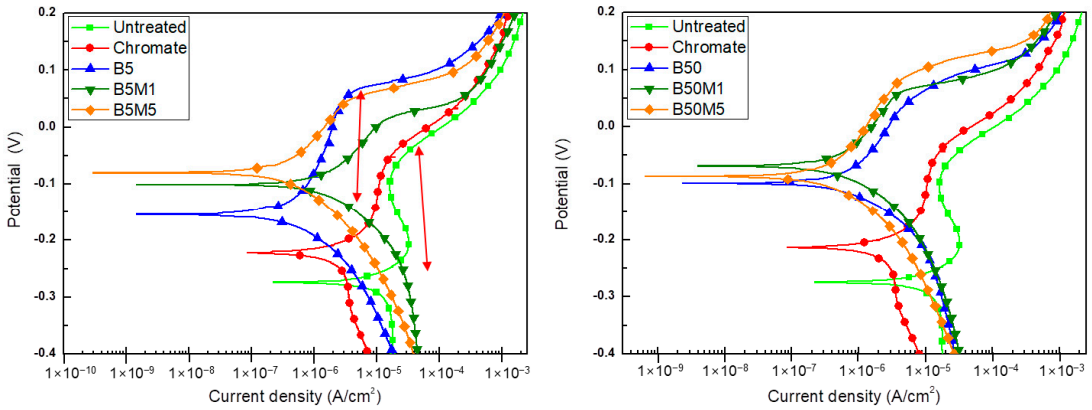

Figure 2. Potentiodynamic polarization curves of surface treatment immersed for 5 s in (**a**) 5 mM and (**b**) 50 mM 1,2,3-benzotriazole (BTA) combined with sodium molybdate (Na_2MoO_4)

A passive film was clearly observed after immersion for 5 s for all BTA-treated groups and $CuMoO_4$ and BTA-Cu synthesized from BTA enhanced the stability of the passive film. In the part of anodic current curve, the breakdown potential was shown with higher anodic current. Passivity means that a thin surface film is formed in the anode polarization to have corrosion resistance. If the cathodic reduction reaction current density is greater than the critical anodic current density, the passive state is stable. In other words, it is a section showing stable current density with increasing potential due to the protective film [35]. Since the thickness of the passive film obtained by anodic polarization was limited to a few nanometers [36], corrosion of the fitting occurred on the surface while the potential increases and the current density raised again as the passive film was destroyed.

After the copper foil was immersed in the surface-treatment solution, the reaction of the insoluble Cu-BTA film started on the surface and it reached an equilibrium reaction at a certain thickness. In other words, 5 s provided sufficient time for the formation of the Cu-BTA film and for the reaction to reach equilibrium. Longer treatment time (i.e., 5 s) provided increased corrosion potential owing to the thicker Cu-BTA film. In other words, setting optimum conditions for both Na_2MoO_4 content and treatment time effectively increased the corrosion potential and reduced the corrosion rate.

3.2. Anti-Discoloration Characteristic

Figure 3a shows the color difference ΔE^* measured after samples underwent the wet condition discoloration test. The chromate group exhibited excellent moisture resistance and has the lowest color

difference ΔE^*. Color difference tended to decrease with increasing deposition time and the addition of Na_2MoO_4. An improvement in moisture resistance was not observed with increasing BTA addition. Although electrochemical corrosion resistance in the Na_2MoO_4 + BTA treated groups was higher than in the chromate group, humidity resistance was lower.

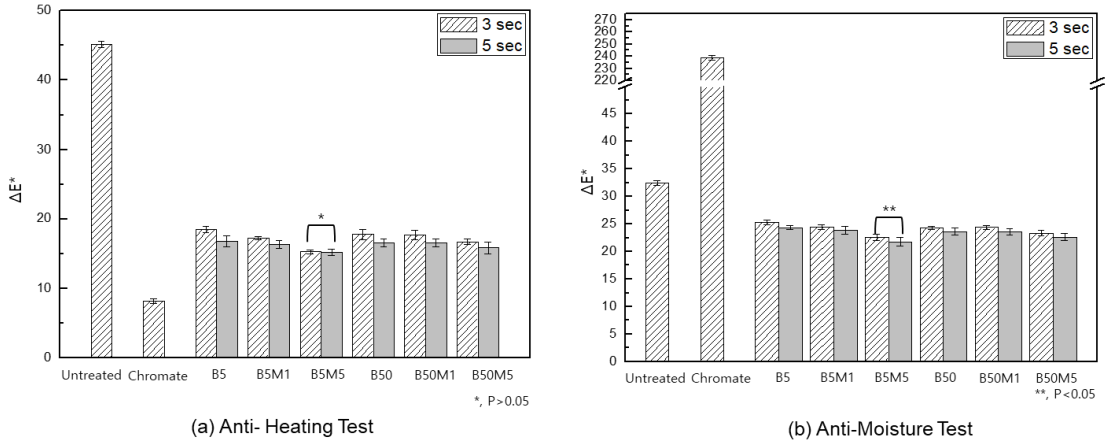

Figure 3. Color difference (ΔE^*) data from discoloration tests under (**a**) high-humidity (80% humidity at 80 °C for 100 h) and (**b**) high-temperature (180 °C for 10 min) conditions.

Chromate samples maintained the same pink surface color after 100 h of moisture resistance evaluation (Figure 4). Chromate with a yellow to pink color has a thickness of just a few microns and the total Cr in the film is just 1.3–1.6 mg·dm^{-2} for gloss [37]. The untreated group and the BTA surface-treatment groups formed local corrosion in the form of black CuCl and copper oxide (II) CuO spots on the copper surface [38]. These spots formed most frequently in the untreated sample and the amounts and sizes of the spots decreased with the addition of Na_2MoO_4.

Figure 3b shows the color difference ΔE^* measured after heat resistance discoloration tests under severe conditions. The chromate sample showed the highest value of discoloration (a ΔE^* value of more than 10 times that of the other groups and a color change from pink to green-blue in Figure 4), followed by the untreated group. The BTA modified groups showed the best heat resistance characteristics. Among the surface-treatment groups using BTA, heat discoloration resistance increased with increasing Na_2MoO_4. This result was similar to that of the electrochemical analysis, which showed relatively better corrosion potential when Na_2MoO_4 was added. During high-temperature testing, the Cr component of a copper surface reacts with O, N and other airborne elements. Owing to the formation of binary compounds (Cr_2O_3 and CrN) with an oxidation state of +3, the chemical bonding of Cr is altered, which may cause a change in the color of the surface [39]. Furthermore, when chromate treatment was carried out at 70 °C or higher, corrosion resistance reduced, and, its corrosion resistance was badly deteriorated at 80 °C. Therefore, when the temperature exceeds 70 °C, fine uniformity occurs in the chromate film causing corrosion and color change [40].

There was no difference in the BTA concentrations for the heat and moisture resistance tests and the results were proportional to the amount of Na_2MoO_4. In terms of moisture resistance, BTA treatment and Na_2MoO_4 addition were lower than those required for the chromate group but higher than those for the untreated group. In particular, thermal resistance was greater than that of the chromate group and the untreated group. Therefore, treatment of BTA with Na_2MoO_4 is effective for surface treatment that requires environmentally friendly heat resistance.

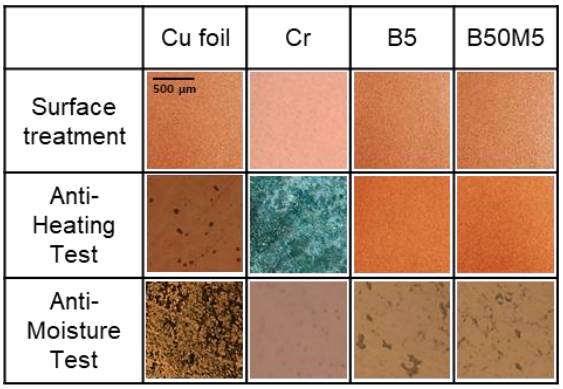

Figure 4. Optical images of Cu foil surfaces after surface treatment and harsh-environment (high humidity and high temperature) tests.

3.3. Surface Morphology Analysis

Morphology analysis based on cross-sections observed by FE-SEM (Figure 5) showed that films prepared by adding Na_2MoO_4 were more densely attached to the Cu substrate and a uniform considering the standard deviation of the thickness data. This was because Na_2MoO_4 accelerated the formation of Cu-BTA, even at relatively low concentrations (1 mM of Na_2MoO_4).

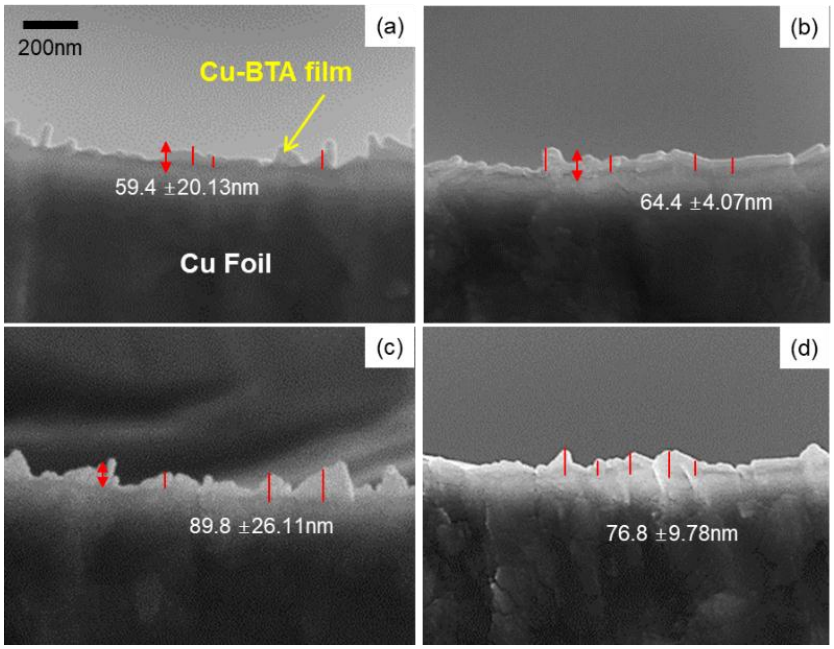

Figure 5. Field emission scanning electron microscopy (FE-SEM) images of sample cross sections: (**a**) B5, (**b**) B5M1, (**c**) B50 and (**d**) B50M1 immersed for 5 s.

In XPS analysis (Figure 6), all of the groups (irrespective of Na_2MoO_4 content) contained C 1*s*, N 1*s*, O 1*s*, Cu 3*d*, Cu 3*p* 1/2, Cu 3*s* and Cu 2*p* 1/2 peaks. The C, N, O elements were components of the BTA and the peaks related to Cu-BTA formation [25]. When 1 mM Na_2MoO_4 was added, Mo-related peaks were not detected in the surface components (binding energy = 228 eV: Mo 3*d* 5/2, 231 eV: Mo 3*d* 3/2, Figure 6(b1)), suggesting that Na_2MoO_4 was involved in the formation of the Cu-BTA film but was not itself part of the chemical bonding [25]. By the way, after treatment with 5 mM Na_2MoO_4, Mo was present in the film and directly involved in corrosion (binding energy = 228 eV: Mo 3*d* 5/2, 231 eV: Mo 3*d* 3/2).

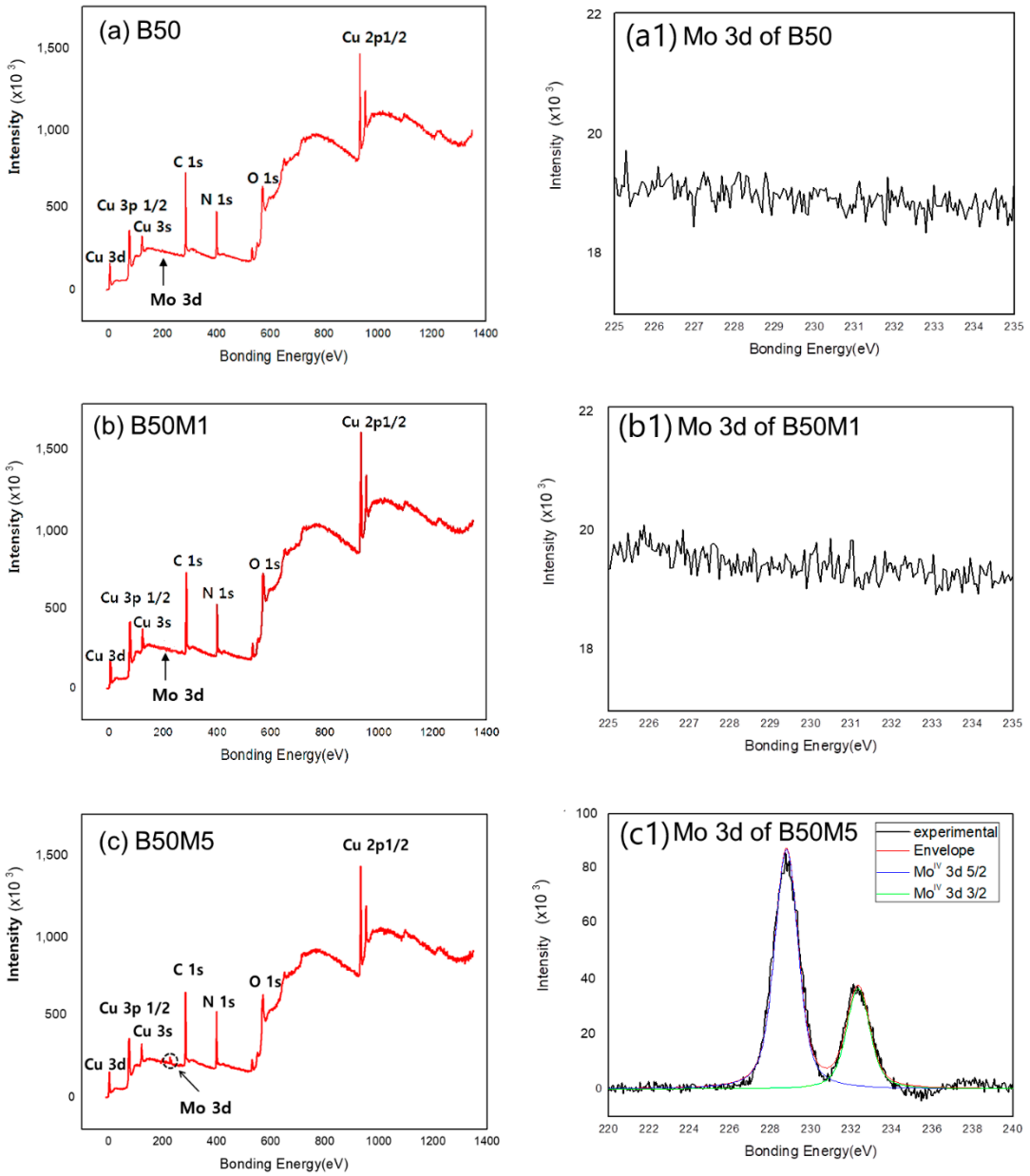

Figure 6. X-ray photoelectron spectroscopy (XPS) patterns of the (**a**) B50, (**b**) B50M1 and (**c**) B50M5 groups immersed for 5 s and XPS spectra of Mo 3*d* (same sample as survey) from each group.

After MoO_4 is reduced to $MoO(OH)_2$, it oxidizes and adheres to intermetallic compound particles [41]. The anion MoO_4^{2-} is preferentially adsorbed on the metal surface to inhibit the entry of chloride ions, thus effectively inhibiting corrosion. In Figure 6(c1), a new Mo 3*d* peaks were observed around the binding energy of 228 eV and 231 eV [42], which can be attributed to Mo in Na_2MoO_4 [43]. This would strengthen the inhibition of BTA on Cu. Na_2MoO_4 itself did not join the inhibition film but promoted the adsorption of BTA at the Cu_2O bottom layer, which is beneficial for the formation of Cu(I) BTA films.

4. Conclusions

This study investigated the influence of additive Na_2MoO_4 and surface-treatment time on the use of BTA as a surface treatment to improve the corrosion resistance and discoloration resistance of the electrolytic copper foil. The corrosion resistances of 5 mM BTA and 50 mM BTA groups were

not effective following 3 s treatment, however the corrosion resistance also increased owing to the formation of a thicker Cu-BTA film as the surface-treatment time increased. In contrast, the addition of Na_2MoO_4 greatly improved the corrosion resistance and the ridging property even after a short treatment time. The increase in the concentration of Na_2MoO_4 was promoted by the adsorption of Cu ions onto the surface of the Cu layer, which is beneficial for the formation of Cu(I) BTA films. It was preferentially adsorbed on the Cu surface where it inhibited the entry of the chloride ions that cause corrosion. Therefore, the surface treatment using Na_2MoO_4 and BTA, which control the concentration and the treatment time, has better discoloration characteristics than the chromate treatment in high temperature (heat resistance) environment, so it is expected to be used in the surface treatment requiring environment-friendly heat resistance.

Author Contributions: Conceptualization, D.-J.S. and I.-S.P.; Methodology, Y.-K.K.; Formal Analysis, D.-J.S. and Y.-K.K.; Writing-Original Draft Preparation D.-J.S. and Y.-K.K.; Writing-Review & Editing, Y.-K.K. and J.-M.Y.; Visualization, I.-S.P.; Supervision, J.-M.Y.; Project Administration, J.-M.Y.; Funding Acquisition, I.-S.P.

Funding: This research was supported by "Research Base Construction Fund Support Program" funded by Chonbuk National University in 2018.

Acknowledgments: This study has reconstructed the data of Dong-Jun Shin's master thesis.

Conflicts of Interest: The authors declare no conflict of interest.

References

1. Weiss, B.; Gröger, V.; Khatibi, G.; Kotas, A.; Zimprich, P.; Stickler, R.; Zagar, B. Characterization of mechanical and thermal properties of thin Cu foils and wires. *Sens. Actuators A Phys.* **2002**, *99*, 172–182. [CrossRef]
2. Merchant, H.D.; Minor, M.G.; Liu, Y.L. Mechanical fatigue of thin copper foil. *J. Electron. Mater.* **1999**, *28*, 998–1007. [CrossRef]
3. De Angelis, R.; Knorr, D.; Merchant, H. Through-thickness characterization of copper electrodeposit. *J. Electron. Mater.* **1995**, *24*, 927. [CrossRef]
4. Merchant, H.D.; Liu, W.C.; Giannuzzi, L.A.; Morris, J.G. Grain structure of thin electrodeposited and rolled copper foils. *Mater. Charact.* **2004**, *53*, 335–360. [CrossRef]
5. FitzGerald, K.P.; Nairn, J.; Skennerton, G.; Atrens, A. Atmospheric corrosion of copper and the colour, structure and composition of natural patinas on copper. *Corros. Sci.* **2006**, *48*, 2480–2509. [CrossRef]
6. Rickett, B.I.; Payer, J.H. Composition of copper tarnish products formed in moist air with trace levels of pollutant gas: Sulfur dioxide and sulfur dioxide/nitrogen dioxide. *J. Electrochem. Soc.* **1995**, *142*, 3713–3722. [CrossRef]
7. Watanabe, M.; Tomita, M.; Ichino, T. Analysis of tarnish films on copper exposed in hot spring area. *J. Electrochem. Soc.* **2002**, *149*, B97–B102. [CrossRef]
8. Kajiwara, T.; Tanii, Y.; Hashimoto, K. Method of Making Thin Copper Foil for Printed Wiring Board. U.S. Patent 5,114,543 A, 19 May 1992.
9. Yamanishi, K.; Oshima, H.; Sakaguchi, K. Copper Foil for Printed Circuits and Process for Producing the Same. U.S. Patent 5,366,814 A, 22 November 1994.
10. Morisaki, S.; Mase, K. Copper Foil Having Bond Strength. U.S. Patent 4,010,005 A, 1 March 1977.
11. Hua, L.; Chan, Y.C.; Wu, Y.P.; Wu, B.Y. The determination of hexavalent chromium (Cr^{6+}) in electronic and electrical components and products to comply with RoHS regulations. *J. Hazard. Mater.* **2009**, *163*, 1360–1368. [CrossRef]
12. Zucchi, F.; Trabanelli, G.; Monticelli, C. The inhibition of copper corrosion in 0.1 M NaCl under heat exchange conditions. *Corros. Sci.* **1996**, *38*, 147–154. [CrossRef]
13. Finšgar, M.; Milošev, I. Inhibition of copper corrosion by 1,2,3-benzotriazole: A review. *Corros. Sci.* **2010**, *52*, 2737–2749. [CrossRef]
14. Ishida, H.; Johnson, R. The inhibition of copper corrosion by azole compounds in humid environments. *Corros. Sci.* **1986**, *26*, 657–667. [CrossRef]
15. Xu, Z.; Lau, S.; Bohn, P.W. The role of benzotriazole in corrosion inhibition: Formation of an oriented monolayer on Cu_2O. *Surf. Sci.* **1993**, *296*, 57–66. [CrossRef]

16. Shams El Din, A.M.; Mohammed, R.A.; Haggag, H.H. Corrosion inhibition by molybdate/polymaliate mixtures. *Desalination* **1997**, *114*, 85–95. [CrossRef]
17. Ramesh, S.; Rajeswari, S.; Maruthamuthu, S. Corrosion inhibition of copper by new triazole phosphonate derivatives. *Appl. Surf. Sci.* **2004**, *229*, 214–225. [CrossRef]
18. Gelman, D.; Starosvetsky, D.; Ein-Eli, Y. Copper corrosion mitigation by binary inhibitor compositions of potassium sorbate and benzotriazole. *Corros. Sci.* **2014**, *82*, 271–279. [CrossRef]
19. Villamil, R.; Corio, P.; Rubim, J.; Agostinho, S. Sodium dodecylsulfate–benzotriazole synergistic effect as an inhibitor of processes on copper | chloridric acid interfaces. *J. Electroanal. Chem.* **2002**, *535*, 75–83. [CrossRef]
20. Saremi, M.; Dehghanian, C.; Sabet, M.M. The effect of molybdate concentration and hydrodynamic effect on mild steel corrosion inhibition in simulated cooling water. *Corros. Sci.* **2006**, *48*, 1404–1412. [CrossRef]
21. Vukasovich, M.S.; Farr, J.P.G. Molybdate in corrosion inhibition—A review. *Polyhedron* **1986**, *5*, 551–559. [CrossRef]
22. Ramesh, S.; Rajeswari, S. Evaluation of inhibitors and biocide on the corrosion control of copper in neutral aqueous environment. *Corros. Sci.* **2005**, *47*, 151–169. [CrossRef]
23. Mustafa, C.; Shahinoor Islam Dulal, S. Molybdate and nitrite as corrosion inhibitors for copper-coupled steel in simulated cooling water. *Corrosion* **1996**, *52*, 16–22. [CrossRef]
24. Deyab, M.A.; Abd El-Rehim, S.S. Inhibitory effect of tungstate, molybdate and nitrite ions on the carbon steel pitting corrosion in alkaline formation water containing Cl^- ion. *Electrochim. Acta* **2007**, *53*, 1754–1760. [CrossRef]
25. Zhang, D.-Q.; Joo, H.G.; Lee, K.Y. Investigation of molybdate–benzotriazole surface treatment against copper tarnishing. *Surf. Interface Anal.* **2009**, *41*, 164–169. [CrossRef]
26. Yang, J.-S.; Lim, S.-L.; Kim, S.-B.; Kim, K.-J. Electrolyte Solution for Manufacturing Electrolytic Copper Foil and Electrolytic Copper Foil Manufacturing Method Using the Same. U.S. Patent 20040104117A1, 3 June 2004.
27. Stansbury, E.E.; Buchanan, R.A. Kinetics of Single Half-Cell Reactions. In *Fundamentals of Electrochemical Corrosion*; Stansbury, E.E., Buchanan, R.A., Eds.; ASM International: Novelty, OH, USA, 2000.
28. Bard, A.J.; Faulkner, L.R.; Leddy, J.; Zoski, C.G. *Electrochemical methods: Fundamentals and Applications*; Wiley: Hoboken, NJ, USA, 1980.
29. Domínguez-Crespo, M.A.; Onofre-Bustamante, E.; Torres-Huerta, A.M.; Rodríguez-Gómez, F.J. Morphology and corrosion performance of chromate conversion coatings on different substrates. *J. Mex. Chem. Soc.* **2008**, *52*, 241–248.
30. Jiang, L.; He, Y.; Niu, X.; Li, Y.; Luo, J. Synergetic effect of benzotriazole and non-ionic surfactant on copper chemical mechanical polishing in KIO_4-based slurries. *Thin Solid Films* **2014**, *558*, 272–278. [CrossRef]
31. Finšgar, M.; Lesar, A.; Kokalj, A.; Milošev, I. A comparative electrochemical and quantum chemical calculation study of BTAH and BTAOH as copper corrosion inhibitors in near neutral chloride solution. *Electrochim. Acta* **2008**, *53*, 8287–8297. [CrossRef]
32. Breslin, C.; Treacy, G.; Carroll, W. Studies on the passivation of aluminium in chromate and molybdate solutions. *Corros. Sci.* **1994**, *36*, 1143–1154. [CrossRef]
33. Moshier, W.; Davis, G. Interaction of molybdate anions with the passive film on aluminum. *Corrosion* **1990**, *46*, 43–50. [CrossRef]
34. Zhou, Y.; Zuo, Y.; Lin, B. The compounded inhibition of sodium molybdate and benzotriazole on pitting corrosion of Q235 steel in NaCl + $NaHCO_3$ solution. *Mater. Chem. Phys.* **2017**, *192*, 86–93. [CrossRef]
35. Jones, D.A. *Principles and Prevention of Corrosion*, 2nd ed.; Prentice Hall: Upper Saddle River, NY, USA, 1996; pp. 168–198.
36. Chandrasekaran, M. Metals for Biomedical Devices. In *Forging of Metals and Alloys for Biomedical Applications*; Niinomi, M., Ed.; Woodhead Publishing: Cambridge, UK, 2010; pp. 235–250.
37. Kim, S.W.; Lee, C.T. Environment-friendly trivalent chromate treatment for Zn electroplating. *J. Korean Ind. Eng. Chem.* **2006**, *17*, 433.
38. Youda, R.; Nishihara, H.; Aramaki, K. SERS and impedance study of the equilibrium between complex formation and adsorption of benzotriazole and 4-hydroxybenzotriazole on a copper electrode in sulphate solutions. *Electrochim. Acta* **1990**, *35*, 1011–1017. [CrossRef]
39. Dorward, R.C.; Hasse, K.R. Incubation effects in precracked stress corrosion specimens from Al-Zn-Mg-Cu alloy 7075. *Corros. Sci.* **1979**, *19*, 131–140. [CrossRef]

40. Laget, V.; Jeffcoate, C.; Isaacs, H.; Buchheit, R. Dehydration-induced loss of corrosion protection properties in chromate conversion coatings on aluminum alloy 2024-T3. *J. Electrochem. Soc.* **2003**, *150*, B425–B432. [CrossRef]
41. Lopez-Garrity, O.; Frankel, G. Corrosion inhibition of aluminum alloy 2024-T3 by sodium molybdate. *J. Electrochem. Soc.* **2014**, *161*, C95–C106. [CrossRef]
42. Zhang, B.; Wu, J.; Peng, D.; Li, X.; Huang, Y. In-Situ Scanning Micro-Electrochemical Characterization of Corrosion Inhibitors on Copper. Available online: https://dr.ntu.edu.sg/handle/10220/40846 (accessed on 26 October 2018).
43. Mert, B.D.; Mert, M.E.; Kardaş, G.; Yazıcı, B. Experimental and theoretical investigation of 3-amino-1,2, 4-triazole-5-thiol as a corrosion inhibitor for carbon steel in HCl medium. *Corros. Sci.* **2011**, *53*, 4265–4272. [CrossRef]